Thermo-optic dispersion formulas for YCOB and GdCOB laser host crystals

Pavel Loiko,[1] Xavier Mateos,[2,*] Yicheng Wang,[3] Zhongben Pan,[4] Konstantin Yumashev,[1] Huaijin Zhang,[5] Uwe Griebner,[3] and Valentin Petrov[3]

[1]*Center for Optical Materials and Technologies, Belarusian National Technical University, 65/17 Nezavisimosti Ave., 220013 Minsk, Belarus*

[2]*Física i Cristal·lografia de Materials i Nanomaterials (FiCMA-FiCNA), Universitat Rovira i Virgili (URV), Campus Sescelades, c/ Marcel·lí Domingo, s/n., Tarragona, E-43007 Spain*

[3]*Max Born Institute for Nonlinear Optics and Short Pulse Spectroscopy, Max-Born-Str. 2a, D-12489 Berlin, Germany*

[4]*Institute of Chemical Materials and Advanced Materials Center, China Academy of Engineering Physics, Mianyang 621900, China*

[5]*State Key Laboratory of Crystal Materials and Institute of Crystal Materials, Shandong University, Jinan 250100, China*

[*]*xavier.mateos@urv.cat*

Abstract: We report on a comparative study of anisotropy and dispersion of thermo-optic coefficients, dn/dT, and thermal coefficients of the optical path for monoclinic oxoborate YCOB and GdCOB laser host crystals. Near 1 μm, all dn/dT coefficients are found to be negative: dn_X/dT = –1.2, dn_Y/dT = –3.7 and dn_Z/dT = –2.5 × 10^{-6} K^{-1} for YCOB, dn_X/dT = –3.8, dn_Y/dT = –4.8 and dn_Z/dT = –3.7 × 10^{-6} K^{-1} for GdCOB. Thermo-optic dispersion formulas are derived for these crystals in the spectral range of 0.4–2 μm. The existence of athermal directions is predicted for both YCOB and GdCOB.

©2015 Optical Society of America

OCIS codes: (160.1190) Anisotropic optical materials; (140.6810) Thermal effects; (260.1180) Crystal optics

References and links

1. F. Mougel, G. Aka, A. Kahn-Harari, H. Hubert, J. M. Benitez, and D. Vivien, "Infrared laser performance and self-frequency doubling of Nd^{3+}:$Ca_4GdO(BO_3)_3$ (Nd:GdCOB)," Opt. Mater. **8**(3), 161–173 (1997).
2. D. A. Hammons, M. Richardson, B. H. T. Chai, A. K. Chin, and R. Jollay, "Scaling of longitudinally diode-pumped self-frequency-doubling Nd:YCOB lasers," IEEE J. Quantum Electron. **36**(8), 991–999 (2000).
3. H. Zhang, X. Meng, P. Wang, L. Zhu, X. Liu, R. Cheng, J. Dawes, P. Dekker, S. Zhang, and L. Sun, "Slope efficiency of up to 73% for Yb:$Ca_4YO(BO_3)_3$ crystal laser pumped by a laser diode," Appl. Phys. B **68**(6), 1147–1149 (1999).
4. F. Druon, F. Balembois, P. Georges, A. Brun, A. Courjaud, C. Hönninger, F. Salin, A. Aron, F. Mougel, G. Aka, and D. Vivien, "Generation of 90-fs pulses from a mode-locked diode-pumped Yb^{3+}:$Ca_4GdO(BO_3)_3$ laser," Opt. Lett. **25**(6), 423–425 (2000).
5. A. Yoshida, A. Schmidt, V. Petrov, C. Fiebig, G. Erbert, J. Liu, H. Zhang, J. Wang, and U. Griebner, "Diode-pumped mode-locked Yb:YCOB laser generating 35 fs pulses," Opt. Lett. **36**(22), 4425–4427 (2011).
6. O. H. Heckl, C. Kränkel, C. R. E. Baer, C. J. Saraceno, T. Südmeyer, K. Petermann, G. Huber, and U. Keller, "Continuous-wave and modelocked Yb:YCOB thin disk laser: first demonstration and future prospects," Opt. Express **18**(18), 19201–19208 (2010).
7. P. Wang, J. M. Dawes, P. Burns, J. A. Piper, H. Zhang, L. Zhu, and X. Meng, "Diode-pumped cw tunable Er^{3+}:Yb^{3+}:YCOB laser at 1.5–1.6 μm," Opt. Mater. **19**, 383–387 (2002).
8. M. Iwai, T. Kobayashi, H. Furuya, Y. Mori, and T. Sasaki, "Crystal growth and optical characterization of rare-earth (Re) calcium oxyborate $ReCa_4O(BO_3)_3$ (Re = Y or Gd) as new nonlinear optical material," Jpn. J. Appl. Phys. **36**(Part 2, No. 3A), L276–L279 (1997).
9. G. Aka, A. Kahn-Harari, F. Mougel, D. Vivien, F. Salin, P. Coquelin, P. Colin, D. Pelenc, and J. P. Damelet, "Linear- and nonlinear-optical properties of a new gadolinium calcium oxoborate crystal, $Ca_4GdO(BO_3)_3$," J. Opt. Soc. Am. B **14**(9), 2238–2247 (1997).
10. F. Mougel, K. Dardenne, G. Aka, A. Kahn-Harari, and D. Vivien, "Ytterbium-doped $Ca_4GdO(BO_3)_3$: an efficient infrared laser and self-frequency doubling crystal," J. Opt. Soc. Am. B **16**(1), 164–172 (1999).
11. Q. Ye and B. H. T. Chai, "Crystal growth of $YCa_4O(BO_3)_3$ and its orientation," J. Cryst. Growth **197**(1-2), 228–235 (1999).

#233231 - $15.00 USD Received 27 Jan 2015; revised 31 Mar 2015; accepted 3 Apr 2015; published 15 Apr 2015

Репозиторий БНТУ

12. F. Mougel, A. Kahn-Harari, G. Aka, and D. Pelenc, "Structural and thermal stability of Czochralski grown GdCOB oxoborate single crystals," J. Mater. Chem. **8**(7), 1619–1623 (1998).
13. J. Luo, S. J. Fan, H. Q. Xie, K. C. Xiao, S. X. Qian, Z. W. Zhong, G. X. Qian, R. Y. Sun, and J. Y. Xu, "Thermal and nonlinear optical properties of $Ca_4YO(BO_3)_3$," Cryst. Res. Technol. **36**(11), 1215–1221 (2001).
14. S. Chenais, F. Druon, S. Forget, F. Balembois, and P. Georges, "On thermal effects in solid-state lasers: The case of ytterbium-doped materials," Prog. Quantum Electron. **30**(4), 89–153 (2006).
15. P. Segonds, B. Boulanger, B. Menaert, J. Zaccaro, J. P. Salvestrini, M. D. Fontana, R. Moncorge, F. Poree, G. Gadret, J. Mangin, A. Brenier, G. Boulon, G. Aka, and D. Pelenc, "Optical characterizations of $YCa_4O(BO_3)_3$ and $Nd:YCa_4O(BO_3)_3$ crystals," Opt. Mater. **29**(8), 975–982 (2007).
16. M. Abarkan, J. P. Salvestrini, D. Pelenc, and M. D. Fontana, "Electro-optic, thermo-optic, and dielectric properties of YCOB and Nd:YCOB crystals: comparative study," J. Opt. Soc. Am. B **22**(2), 398–406 (2005).
17. S. Chénais, F. Balembois, F. Druon, G. Lucas-Leclin, and P. Georges, "Thermal lensing in diode-pumped ytterbium lasers – Part II: Evaluation of quantum efficiencies and thermo-optic coefficients," IEEE J. Quantum Electron. **40**(9), 1235–1243 (2004).
18. Y. Petit, S. Joly, P. Segonds, and B. Boulanger, "Recent advances in monoclinic crystal optics," Laser and Photon. Rev. **7**(6), 920–937 (2013).
19. S. Vatnik, M. C. Pujol, J. J. Carvajal, X. Mateos, M. Aguiló, F. Díaz, and V. Petrov, "Thermo–optic coefficients of monoclinic $KLu(WO_4)_2$," Appl. Phys. B **95**(4), 653–656 (2009).
20. L. Palfalvi and J. Hebling, "Z-scan study of the thermo-optical effect," Appl. Phys. B **78**, 775–780 (2004).
21. E. Koushki and A. Farzaneh, "Time dependence of thermo-optical effect for thin samples containing light-absorptive material," Opt. Commun. **285**(6), 1390–1393 (2012).
22. P. Loiko, F. Druon, P. Georges, B. Viana, and K. Yumashev, "Thermo-optic characterization of $Yb:CaGdAlO_4$ laser crystal," Opt. Mater. Express **4**(11), 2241–2249 (2014).
23. P. A. Loiko, K. V. Yumashev, N. V. Kuleshov, and A. A. Pavlyuk, "Thermooptic coefficients of Nd-doped anisotropic $KGd(WO_4)_2$, YVO_4 and $GdVO_4$ laser crystals," Appl. Phys. B **102**(1), 117–122 (2011).
24. C. Wang, H. Zhang, X. Meng, L. Zhu, Y. T. Chow, X. Liu, R. Cheng, Z. Yang, S. Zhang, and L. Sun, "Thermal, spectroscopic properties and laser performance at 1.06 and 1.33 μm of $Nd:Ca_4YO(BO_3)_3$ and $Nd:Ca_4GdO(BO_3)_3$ crystals," J. Cryst. Growth **220**(1-2), 114–120 (2000).
25. J. Zhou, Z. Zhong, J. Xu, J. Luo, W. Hua, and S. Fan, "Bridgman growth and characterization of nonlinear optical single crystals $Ca_4GdO(BO_3)_3$," Mater. Sci. Eng. B **97**(3), 283–287 (2003).
26. J. J. Zayhowski and A. Mooradian, "Single-frequency microchip Nd lasers," Opt. Lett. **14**(1), 24–26 (1989).
27. J. M. Serres, X. Mateos, P. Loiko, K. Yumashev, N. Kuleshov, V. Petrov, U. Griebner, M. Aguiló, and F. Díaz, "Diode-pumped microchip $Tm:KLu(WO_4)_2$ laser with more than 3 W of output power," Opt. Lett. **39**(14), 4247–4250 (2014).
28. P. A. Loiko, K. V. Yumashev, N. V. Kuleshov, G. E. Rachkovskaya, and A. A. Pavlyuk, "Thermo-optic dispersion formulas for monoclinic double tungstates $KRe(WO_4)_2$ where *Re* = Gd, Y, Lu, Yb," Opt. Mater. **33**(11), 1688–1694 (2011).
29. R. N. Abbott, Jr., "Calculation of the orientation of the optical indicatrix in monoclinic and triclinic crystals: The point-dipole model," Am. Mineral. **78**, 952–956 (1993).
30. C. Traum, P. L. Inácio, C. Félix, P. Segonds, A. Peña, J. Debray, B. Boulanger, Y. Petit, D. Rytz, G. Montemezzani, P. Goldner, and A. Ferrier, "Direct measurement of the dielectric frame rotation of monoclinic crystals as a function of the wavelength," Opt. Mater. Express **4**(1), 57–62 (2014).
31. G. Ghosh, *Handbook of Thermo–optic Coefficients of Optical Materials with Applications* (Academic Press, 1998).
32. P. A. Loiko, K. V. Yumashev, N. V. Kuleshov, and A. A. Pavlyuk, "Thermo-optical properties of pure and Yb-doped monoclinic $KY(WO_4)_2$ crystals," Appl. Phys. B **106**(3), 663–668 (2012).
33. P. A. Loiko, X. Han, K. V. Yumashev, N. V. Kuleshov, M. D. Serrano, C. Cascales, and C. Zaldo, "Thermo-optical properties of uniaxial $NaT(XO_4)_2$ laser host crystals (where T = Y, La, Gd or Bi and X = W or Mo)," Appl. Phys. B **111**(2), 279–287 (2013).
34. H. J. Zhang, H. D. Jiang, J. Y. Wang, X. B. Hu, G. W. Yu, W. T. Yu, L. Gao, J. A. Liu, S. J. Zhang, and M. H. Jiang, "Growth and characterization of a $LaCa_4O(BO_3)_3$ crystal," Appl. Phys., A Mater. Sci. Process. **78**(6), 889–893 (2004).
35. H.-R. Xia, M. Guo, H.-D. Jiang, J.-Y. Wang, J.-Q. Wei, X.-B. Hu, B. Gong, and Y.-G. Liu, "Self-frequency doubled green $Nd_xY_{1-x}Ca_4O(BO_3)_3$ laser," Phys. Status Solidi **183**(2), 427–434 (2001) (a).
36. P. A. Loiko, V. V. Filippov, K. V. Yumashev, N. V. Kuleshov, and A. A. Pavlyuk, "All-space existence and dispersion of athermal directions in monoclinic $KY(WO_4)_2$," Opt. Commun. **326**, 144–149 (2014).
37. S. Biswal, S. P. O'Connor, and S. R. Bowman, "Thermo-optical parameters measured in ytterbium-doped potassium gadolinium tungstate," Appl. Opt. **44**(15), 3093–3097 (2005).

1. Introduction

Monoclinic, point group *m*, calcium rare-earth oxoborate crystals like $Ca_4YO(BO_3)_3$ (YCOB) and $Ca_4GdO(BO_3)_3$ (GdCOB) doped with Nd^{3+} trivalent ions are well established laser materials [1,2]. Efficient continuous-wave, Q-switched and mode-locked Yb:YCOB and Yb:GdCOB lasers were reported [3–5]; in the last case generating pulses as short as 35 fs [5]. Recently, thin disk lasers [6] were also realized with Yb:YCOB, including mode-locked

#233231 - $15.00 USD Received 27 Jan 2015; revised 31 Mar 2015; accepted 3 Apr 2015; published 15 Apr 2015
(C) 2015 OSA

Репозиторий БНТУ

operation. Eye-safe Er,Yb:YCOB lasers were studied as well [7]. The noncentrosymmetric oxoborate crystals also show good nonlinear properties [8,9] and are of practical interest for second-harmonic generation (SHG) and (chirped pulse) optical parametric amplification. Moreover, the feasibilty of Yb- [10] and Nd-doped [1,2] oxoborates for self-frequency doubling was also demonstrated which enabled the development of compact green lasers. Both YCOB and GdCOB compounds melt congruently [8,11], so they can be pulled directly from the melt which enables the growth of large-volume crystals. The structure, spectroscopic and nonlinear optical properties of YCOB and GdCOB were widely studied in the past years.

Thermal properties of YCOB and GdCOB are not optimal. This includes a relatively low thermal conductivity (~2 W/mK) [12], and large and strongly anisotropic thermal expansion (up to ~12 × 10^{-6} K^{-1}) [13]. This can lead to high thermal stress that typically causes crystal cracking, and a strong thermal lensing. The latter is the main detrimental effect that limits the power scaling capabilities of solid-state lasers [14]. Indeed, it can lead to cavity instability, degradation of the laser performance and beam quality, and even to ceasing of laser operation. Thermal lens considerations require knowledge of yet more important parameters such as the thermo-optic coefficient (TOC = dn/dT) and thermal coefficient of the optical path (TCOP). Unfortunately, there is a strong discrepancy in the scarce literature on this subject [15–17] concerning these two parameters which are important also in nonlinear optical applications in relation to temperature variation of the refractive index and associated phase mismatching.

In the present paper, we report on a comprehensive comparative study of thermo-optical properties of YCOB and GdCOB, taking into account their intrinsic anisotropy. In addition, the dispersion of dn/dT coefficients is investigated, yielding thermo-optic dispersion formulas for a wide spectral range from 0.4 to 2 μm. The physical effects behind the negative dn/dT values, as well as their potential utilization (athermal behavior) are discussed, too.

2. Experimental

The studied YCOB and GdCOB single crystals were grown by the Czochralsky method. Monoclinic YCOB and GdCOB are biaxial and their optical properties are described in the frame of the optical indicatrix with the three principal axes, X, Y and Z corresponding to refractive indices $n_X < n_Y < n_Z$ [9,15]. The axis corresponding to the medium refractive index, Y, is parallel to the b crystallographic axis. The two remaining axes, X and Z, are located in the a-c plane, see Fig. 1. The orientation of the optical indicatrix (a^Z ~26° and c^X ~15°) of GdCOB is nearly wavelength independent between 0.4 and 2.2 μm [18].

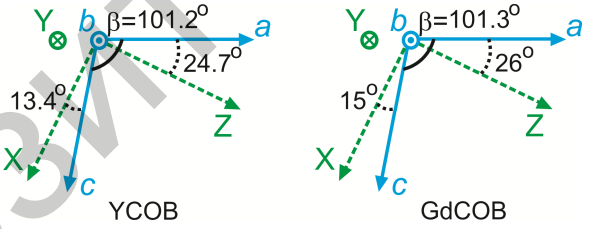

Fig. 1. Orientation of the optical indicatrix (X, Y and Z axes) with respect to the crystallographic frame (a, b and c axes) for monoclinic biaxial YCOB and GdCOB crystals [9,15].

From the as-grown bulk crystals, two rectangular samples were cut in the frame of the optical indicatrix having the dimensions of 6.01(X) × 7.41(Y) × 6.88(Z) mm^3 for YCOB and 6.97(X) × 5.17(Y) × 5.67(Z) mm^3 for GdCOB. All faces of the samples were polished.

Thermal expansion coefficients α for both crystals were measured along the X, Y and Z axes by a horizontal dilatometer, model Netzsch 402PC, for the temperature range RT (room-temperature) – 200 °C, with a precision of 0.1 × 10^{-6} K^{-1}.

TCOPs were measured by the laser beam deviation method for a sample with a linear thermal gradient [19] with a precision of 0.2 × 10^{-6} K^{-1}. To employ this method, two opposite faces of the rectangular samples were maintained at different temperatures (~0 °C for the

#233231 - $15.00 USD Received 27 Jan 2015; revised 31 Mar 2015; accepted 3 Apr 2015; published 15 Apr 2015
(C) 2015 OSA

Репозиторий БНТУ

"cold" surface and ~50 °C for the "hot" one) thus producing a linear thermal gradient of ~6–8 °C/mm. The temperature gradient was applied perpendicularly to the light propagation direction of a probe beam. The probe beam was formed by a telescope, iris and a Glan-Taylor prism to be linearly polarized and to have a nearly flat wave front ("top-hat" profile). The diameter of the probe beam in the sample was ~3 mm. We used a set of continuous-wave lasers emitting at 400, 532, 633, 652, 780, 980 and 1064 nm (laser power was <10 mW). Thus, the intensity of the probe beam was too low to produce any nonlinear effects in the sample [20]. As all wavelengths used were within the transparency range of YCOB and GdCOB, no additional heat was released in the sample by the probe beam [21]. The sample was only loosely fixed (without exerting a pressure) to avoid thermally induced stresses that could in principle modify the refractive index [22]. Under these conditions, a linear thermal gradient corresponds to a linear change of the optical path length. The latter causes a deviation of the probe beam from the straightforward direction. This deviation is proportional to the TCOP ($W = \mathrm{d}n/\mathrm{d}T + (n-1)\alpha$, where α is the thermal expansion along the light propagation direction). Further details about the method used can be found elsewhere [22].

The three possible light propagation directions along the X, Y or Z axes (denoted further as X-, Y- or Z-cut) alongside the two possible principal polarizations yield a total of 6 TCOP values. As oxoborates exhibit anisotropy of the thermal conductivity coefficient κ (in particular, for GdCOB $\kappa_X = 2.17$, $\kappa_Y = 1.32$ and $\kappa_Z = 2.40$ W/mK [12]), the temperature gradient was carefully measured for each sample orientation using a pair of sensitive thermocouples with a precision of ~0.1 °C. Considering the applied temperatures, it can be concluded that all TCOP values were determined at around room-temperature.

The principal TOCs, $\mathrm{d}n_X/\mathrm{d}T$, $\mathrm{d}n_Y/\mathrm{d}T$ and $\mathrm{d}n_Z/\mathrm{d}T$, were determined from the corresponding TCOP values, $\mathrm{d}n/\mathrm{d}T = W-(n-1)\alpha$; the refractive indices n were calculated from Sellmeier equations [9,15]. It is important to note that each $\mathrm{d}n/\mathrm{d}T$ value was determined independently from two measurements like in [23] (for instance, $\mathrm{d}n_X/\mathrm{d}T$ was derived from the data for $E \parallel X$ polarization, Y-cut and Z-cut samples). The coincidence of two $\mathrm{d}n/\mathrm{d}T$ values is then an indicator of the correctness of our method and the deviation did not exceed 0.3×10^{-6} K^{-1}.

3. Results and discussion

The measured thermal expansion coefficients amount to $\alpha_X = 12.0$, $\alpha_Y = 2.6$, $\alpha_Z = 6.2 \times 10^{-6}$ K^{-1} for YCOB, and $\alpha_X = 11.1$, $\alpha_Y = 3.6$ and $\alpha_Z = 7.7 \times 10^{-6}$ K^{-1} for GdCOB, see Table 1 also showing a comparison with previous data. The degree of anisotropy of the thermal expansion, denoted as $\alpha_X:\alpha_Y:\alpha_Z$, is higher for YCOB (4.6:1:2.4) as compared to GdCOB (3.1:1:2.1).

Table 1. Thermal Expansion Coefficients for YCOB and GdCOB Crystals

Crystal	Thermal expansion, 10^{-6} K^{-1}					Ref.
	α_X	α_c	$\alpha_Y = \alpha_b$	α_Z	α_a	
YCOB	12.0		2.6	6.2		This paper
	12.6		4.1	7.5		[15]
		12.8	8.2		9.9	[13]
Nd:YCOB	10.9		4.2	5.9		[24]
	12.1		4.4	7.7		[15]
GdCOB	11.1		3.6	7.7		This paper
		14.3	8.3		10.2	[12]
		13.1	7.8		10.4	[25]
Nd:GdCOB	11.6		5.4	5.9		[24]

The anisotropy and dispersion of the TCOPs are analyzed in Fig. 2. The values at ~1 μm are also compiled in Table 2. For both YCOB and GdCOB crystals, TCOP values can be either positive (X- or Z-cuts) or negative (Y-cut). This means that the sign of the thermal lens which is directly related to the TCOP value [17], will also vary according to the crystal cut. Focusing (positive) thermal lens is then expected for X- or Z-cut YCOB and GdCOB crystals. All TCOP values decrease with the laser wavelength and this dependence is more pronounced at shorter wavelengths.

#233231 - $15.00 USD Received 27 Jan 2015; revised 31 Mar 2015; accepted 3 Apr 2015; published 15 Apr 2015
(C) 2015 OSA

Репозиторий БНТУ

Microchip laser means a gain medium with two flat mirrors directly attached to its faces thus creating a plano-plano cavity without air gaps [26]. The key property of the laser material in this case is the thermal lens sign, as the laser mode is stabilized in the plano-plano cavity only by a positive thermal lens [27]. From this point of view, only X- and Z-cut YCOB and GdCOB crystals are suitable for microchip operation, Table 2.

The difference in TCOP values for the same crystal cut and orthogonal light polarizations, and close emission cross-sections for these polarizations [10] mean that for YCOB or GdCOB lasers, it is in principle possible to observe the so-called polarization-switching effect [22].

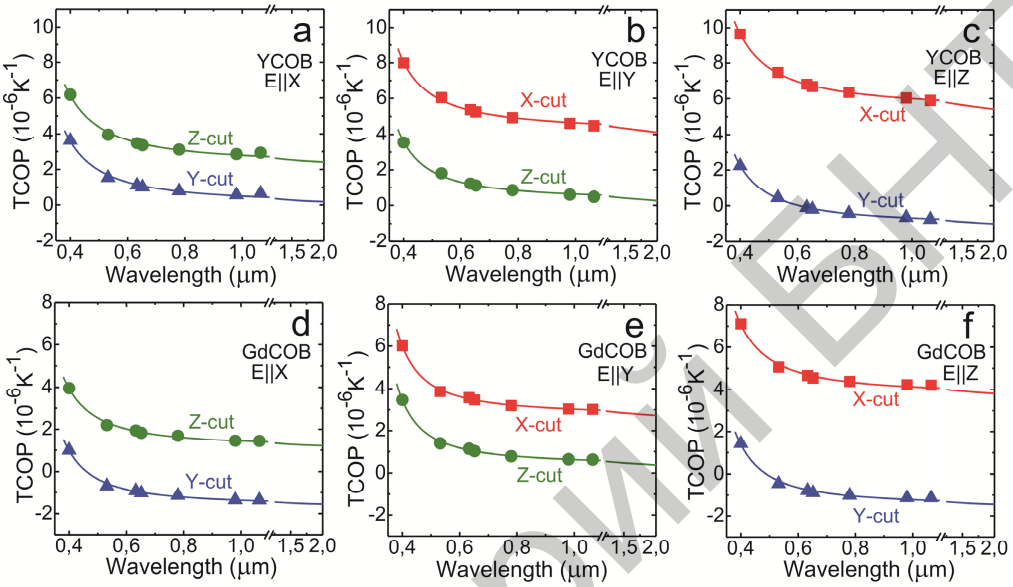

Fig. 2. Dispersion of thermal coefficients of the optical path (TCOP) for YCOB and GdCOB crystals for principal light polarizations $E \parallel X$, Y and Z: *symbols* are the experimental data, *curves* are their fitting.

Table 2. Anisotropy of Thermal Coefficients of the Optical Path (TCOP) for YCOB and GdCOB Crystals at 1.06 μm

Crystal	Orientation	TCOP, 10^{-6} K^{-1}		
		$E \parallel X$	$E \parallel Y$	$E \parallel Z$
YCOB	*X*-cut	–	+ 4.5	+ 5.9
	Y-cut	+ 0.6	–	–0.8
	Z-cut	+ 2.9	+ 0.5	–
GdCOB	*X*-cut	–	+ 3.0	+ 4.2
	Y-cut	–1.4	–	–1.1
	Z-cut	+ 1.4	+ 0.6	–

Different-signed TCOP values for YCOB and GdCOB is a clear indication of negative TOCs (as the impact of the thermal expansion is positive). The dn/dT results are summarized in Fig. 3. At ~1 μm, $dn_X/dT = -1.2$, $dn_Y/dT = -3.7$ and $dn_Z/dT = -2.5 \times 10^{-6}$ K^{-1} for YCOB whereas $dn_X/dT = -3.8$, $dn_Y/dT = -4.8$ and $dn_Z/dT = -3.7 \times 10^{-6}$ K^{-1} for GdCOB (all TOCs are negative). Thus, the anisotropy of temperature dependence of the refractive index is higher for YCOB. All dn/dT values decrease with wavelength. For the entire spectral range studied, the relation $dn_Y/dT < dn_Z/dT < dn_X/dT$ for YCOB and $dn_Y/dT < dn_X/dT < dn_Z/dT$ for GdCOB, holds true. However, no direct link with the relation $n_X < n_Y < n_Z$, exists. This is similar to the behavior observed previously for monoclinic $KGd(WO_4)_2$ and $KY(WO_4)_2$ crystals [28].

Репозиторий БНТУ

#233231 - $15.00 USD Received 27 Jan 2015; revised 31 Mar 2015; accepted 3 Apr 2015; published 15 Apr 2015
(C) 2015 OSA

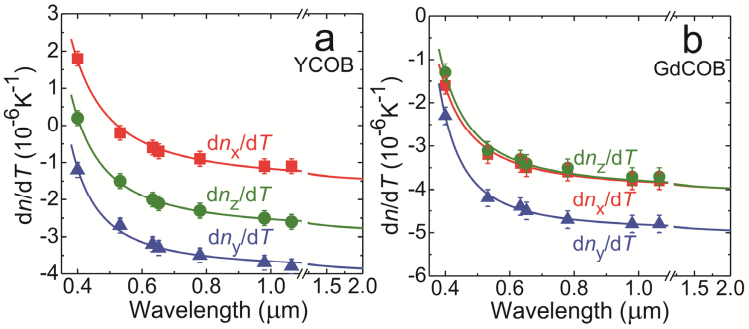

Fig. 3. Dispersion of thermo-optic coefficients, dn_X/dT, dn_Y/dT and dn_e/dT, for YCOB and GdCOB for principal light polarizations $E \parallel X$, Y and Z: *symbols* are the experimental data, *curves* are their fitting.

In Table 3, thermal coefficients of the natural birefringence, $d\Delta/dT$ (defined, e.g. for Z-cut crystal as $d\Delta_{XY}/dT = |dn_X/dT - dn_Y/dT|$ where $\Delta_{XY} = n_X - n_Y$) are presented. The values of $d\Delta/dT$ are relatively small, the maximum variation occurs for Z-cut YCOB as $d\Delta_{XY}/dT = 2.5 \times 10^{-6}$ K^{-1}. In the case of Y-cut GdCOB, $d\Delta_{XZ}/dT$ is almost vanishing.

Table 3. Thermo-Optic Coefficients (TOC) for YCOB and GdCOB Crystals

Crystal	TOC*, 10^{-6} K^{-1}		
	dn_X/dT	dn_Y/dT	dn_Z/dT
YCOB	–1.2	–3.7	–2.5
GdCOB	–3.8	–4.8	–3.7
	$d\Delta_{XY}/dT$**	$d\Delta_{XZ}/dT$	$d\Delta_{YZ}/dT$
YCOB	2.5	1.3	1.2
GdCOB	1.0	0.1	1.1

*At ~1 μm;
**$d\Delta/dT$ is the thermal coefficient of birefringence.

For a monoclinic crystal, the orientation of the optical indicatrix axes is constrained by the crystal symmetry. There are three point groups corresponding to the monoclinic crystal class, namely *2*, *m* and *2/m* (Hermann–Mauguin notations) where *2* stands for a two-fold axis (C_2) and *m* for a mirror plane. A "monoclinic" axis is selected for each point group. This axis is parallel to the two-fold axis for *2* and *2/m* groups and it is perpendicular to the mirror plane for *m* and *2/m* groups. The usual convention is to denote the monoclinic axis as the crystallographic *b*-axis while the angle $\beta = a\hat{}c$ between the *a* and *c* axes located in the orthogonal plane is > 90°, see Fig. 1. The orientation of only one of the principal axes of the optical indicatrix is constrained to be parallel to the *b*-axis. However, as the notations for the axes of the optical indicatrix are determined from the relation for the refractive indices ($n_X < n_Y < n_Z$), any of the X, Y or Z axes may happen to be parallel to the monoclinic axis. It was shown for monoclinic crystals that the values of *n* depend mainly on the electronic polarizabilities of the species occupying the sites, i.e. mainly on the chemical crystal composition [29]. As a result, indeed all three cases (*b* || X, Y or Z) are possible for such crystals [30]. The calculation of *n* is based on the point-dipole model and uses the crystallographic refinement. To date, this approach has not been applied for oxoborates although the crystallographic data are known for these crystals [12].

Thus, to analyze the origin of negative TOCs in oxoborates, we used a recently developed phenomenological model. It does not directly take into account the crystal anisotropy but allows one to model the dn/dT dispersion for the principal polarizations separately which is useful for practical purposes. The model takes into account two main effects, the volumetric thermal expansion (expressed by the α_{vol} value), and the temperature dependence of the electronic bandgap E_g (expressed by a temperature derivative, dE_g/dT) [28,31]:

#233231 - $15.00 USD Received 27 Jan 2015; revised 31 Mar 2015; accepted 3 Apr 2015; published 15 Apr 2015
(C) 2015 OSA

Репозиторий БНТУ

$$\mathrm{d}n/\mathrm{d}T = -\alpha_{\mathrm{vol}}\frac{(n_\infty^2-1)}{2n(\lambda)}\frac{\lambda^2}{\lambda^2-\lambda_g^2} - \frac{1}{E_g}\frac{\mathrm{d}E_g}{\mathrm{d}T}\frac{(n_\infty^2-1)}{2n(\lambda)}\left(\frac{\lambda^2}{\lambda^2-\lambda_g^2}\right)^2. \quad (1)$$

Here λ denotes wavelength; λ_g [μm] = 1.2398/E_g [eV], $n(\lambda)$ is the Sellmeier equation, and n_∞ is the refractive index in the long-wavelength infrared limit. Accordingly, the dn/dT value can be represented as a sum of the terms related to the above mentioned effects, $(\mathrm{d}n/\mathrm{d}T)_\alpha$ + $(\mathrm{d}n/\mathrm{d}T)_g$ [30]. The first term, $(\mathrm{d}n/\mathrm{d}T)_\alpha$, has weaker wavelength dependence and it is negative. Indeed, the crystal volume increases due to volumetric thermal expansion; this decreases the material density and, hence, the refractive index. The second term $(\mathrm{d}n/\mathrm{d}T)_g$ plays the main role for wavelengths close to λ_g near the UV absorption edge and it is positive (as $\mathrm{d}E_g/\mathrm{d}T < 0$).

Using Eq. (1), it is possible to discuss phenomenologically the reasons for the anisotropy of TOCs in monoclinic crystals. The first of them is related to the difference in the band structure (i.e., in the value of electronic bandgap E_g and its temperature-dependence) for the principal light polarizations. This effect was detected for monoclinic double tungstates (E_g was different for light polarized parallel and perpendicular to the C_2-axis) [32]. A second reason is the necessity to consider the anisotropy of the thermal expansion, i.e., to correct the α_{vol} value with "anisotropy" factors. This will be a topic of a separate study.

Negative TOC sign, like observed in YCOB and GdCOB crystals, implies that the impact of the volumetric thermal effect is dominant. However, in the UV region $(\mathrm{d}n/\mathrm{d}T)_g$ exhibits a more abrupt dependence on the wavelength. Thus, at some point the relation $(\mathrm{d}n/\mathrm{d}T)_\alpha = -(\mathrm{d}n/\mathrm{d}T)_g$ holds resulting in zero TOC (meaning a constant refractive index upon heating [33]). This was observed experimentally for YCOB, Fig. 3, and is expected for GdCOB for $\lambda < 0.4$ μm. Such switching of the dn/dT sign was reported previously for monoclinic double tungstates like $KGd(WO_4)_2$ [28] and some nonlinear crystals [31].

Experimental data on the TOCs were fitted with Eq. (1) using α_{vol}, E_g (or λ_g) and $\mathrm{d}E_g/\mathrm{d}T$ as fitting parameters. The best fitting curves are shown in Fig. 3. The α_{vol} value is determined as $\Sigma\alpha'_{ii}$ where α'_{ii} are the diagonal elements of the thermal expansion tensor in its eigen frame. However, as shown in [34], this frame is very close to the optical indicatrix (rotated by an angle φ ~4°), thus α_{vol} was estimated as 20.8 for YCOB and 22.4 × 10^{-6} K^{-1} for GdCOB. Typical values of the remaining fitting parameters are E_g = 5.4 ± 0.1 eV (i.e., close to the value reported in [35], E_g = 5.39 eV) and dE_g/dT = –1.0 ± 0.3 × 10^{-4} eV/K. From the modeling, we conclude that the larger volumetric thermal expansion of GdCOB is responsible for the lower thermo-optic coefficients (as compared with YCOB), Fig. 3.

The performed modeling allows one to derive simple analytical thermo-optic dispersion formulas [33]:

$$\mathrm{d}n/\mathrm{d}T = A_0 + \frac{A_1}{\lambda^2} + \frac{A_2}{\lambda^4} + \frac{A_3}{\lambda^6},\ 10^{-6}\,\mathrm{K}^{-1}. \quad (2)$$

Here λ is in μm; $A_{0\text{-}3}$ are the expansion coefficients (A_0 corresponds to the dn/dT value in the long-wavelength limit, $A_{1\text{-}3}$ represent its dispersion). Their values are listed in Table 4. The equivalence between Eq. (1) and (2) is better than 0.2 × 10^{-6} K^{-1}. Due to a relatively low change in the near-IR region, the curves were extrapolated up to ~2 μm, the region of interest for 1.5-1.6 μm Er lasers [7], as well as Tm/Ho oxoborate crystals that have not been studied to date.

Table 4. Coefficients in the Thermo-Optic Dispersion Formulas for YCOB and GdCOB Crystals, Eq. (2)

Crystal	TOC	A_0	A_1, μm^2	A_2, μm^4	A_3, μm^6
YCOB	dn_X/dT	–1.5	0.3290	0.0137	0.0027
	dn_Y/dT	–3.9	0.2483	–0.0063	0.0059
	dn_Z/dT	–2.8	0.3006	0.0027	0.0044
GdCOB	dn_X/dT	–4.1	0.1937	0.0087	0.0034
	dn_Y/dT	–5.0	0.1808	–0.0082	0.0077
	dn_Z/dT	–4.0	0.2243	0.0058	0.0043

#233231 - $15.00 USD Received 27 Jan 2015; revised 31 Mar 2015; accepted 3 Apr 2015; published 15 Apr 2015
(C) 2015 OSA

Репозиторий БГТУ

Using the Sellmeier equations [9,15] and the obtained thermo-optic dispersion formulas we calculated also the dispersion curves for the TCOP coefficients, see Fig. 2.

Negative TOCs are a prerequisite for the so-called *athermal* behavior [33], with a near-zero variation of the optical path length with temperature. This is achievable when the following relation holds, $W = \mathrm{d}n/\mathrm{d}T + (n-1)\alpha = 0$, called "laser cavity" configuration [34]. We discuss the existence of an athermal direction (AD) for YCOB and GdCOB crystals only for the principal light polarizations, along X, Y or Z axes. For a fixed light polarization E (i.e., constant n and $\mathrm{d}n/\mathrm{d}T$ [36]), the only possibility for the variation of the TCOP value is the change of the α coefficient which depends on the direction of light propagation.

From Table 2, it is clear that for light polarizations $E \parallel$ X and $E \parallel$ Z ADs may exist. Indeed, for these polarizations the sign of the TCOP can be either positive or negative, depending on the light propagation direction. In contrast, for $E \parallel$ Y the TCOP is always positive (no ADs). For $E \parallel$ X, all possible propagation directions lie in the Y-Z plane and for $E \parallel$ Z they are in the X-Y plane. Thus, we calculated the dependence of the TCOP on the propagation direction in both these planes, see Fig. 4, by using the following formulas:

$$W_{\text{Y-Z}} = \mathrm{d}n_{\text{X}} / \mathrm{d}T + (n_{\text{X}} - 1)[\alpha_{\text{Y}} \cos^2\theta + \alpha_{\text{Z}} \sin^2\theta], \quad (3a)$$

$$W_{\text{X-Y}} = \mathrm{d}n_{\text{Z}} / \mathrm{d}T + (n_{\text{Z}} - 1)[\alpha_{\text{Y}} \cos^2\theta + \alpha_{\text{X}} \sin^2\theta]. \quad (3b)$$

Here θ is the angle between the propagation direction and Y axis. The angles corresponding to ADs, θ_{AD}, are then determined from the conditions $W_{\text{Y-Z}} = 0$ (for Y-Z plane) and $W_{\text{X-Y}} = 0$ (for X-Y plane).

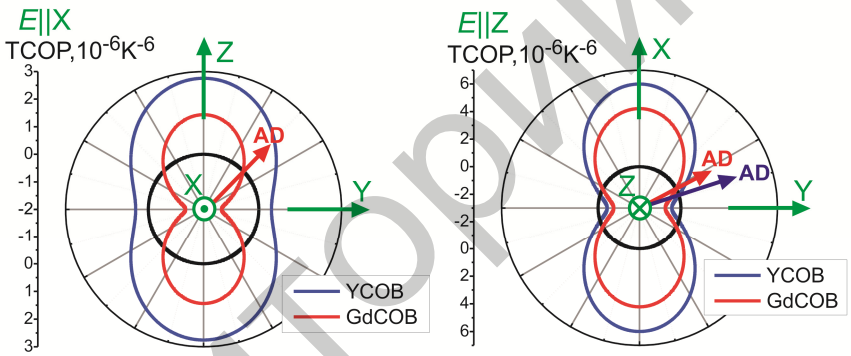

Fig. 4. Analysis of athermal behavior for YCOB and GdCOB crystals at ~1 μm for light polarizations $E \parallel$ X and $E \parallel$ Z: *curves* represent the dependence of the TCOP value on the propagation direction; *black circles* correspond to zero TCOP; *arrows* show athermal directions (ADs).

Table 5. Athermal Directions (ADs) in YCOB and GdCOB Crystals at ~1 μm

Crystal	Polarization (plane)		
	$E \parallel$ X (Y-Z plane)	$E \parallel$ Y (X-Z plane)	$E \parallel$ Z (X-Y plane)
YCOB	–	~Z-axis	Y ± 27.4°
GdCOB	Y ± 43.5°	~Z-axis	Y ± 18.2°

The ADs for YCOB and GdCOB crystals at ~1 μm are summarized in Table 5. In GdCOB, they exist for both $E \parallel$ X and Z polarizations (due to lower $\mathrm{d}n/\mathrm{d}T$ values). ADs are located symmetrically, making angles ± 43.5° (Y-Z plane) and ± 18.2° (X-Y plane) with the Y axis. For YCOB, AD exists only for $E \parallel$ Z, with the orientation Y ± 27.4° in the X-Y plane. As for $E \parallel$ Y polarization, the crystal cut along the Z-axis itself provides a low TCOP, ~0.5 × 10^{-6} K^{-1}, see Table 2. Thus, this axis can be roughly considered as near-athermal direction.

Репозиторий БНТУ

#233231 - $15.00 USD Received 27 Jan 2015; revised 31 Mar 2015; accepted 3 Apr 2015; published 15 Apr 2015
(C) 2015 OSA

4. Conclusions

Monoclinic oxoborate crystals, YCOB and GdCOB, though with relatively low thermal conductivity, provide a beneficial athermal behaviour that should lead to the reduction of the optical power of the thermal lens. This occurs due to negative thermo-optic coefficients in the visible and near-IR, dn/dT, as well as large anisotropy of the thermal expansion effect. Crystal cuts showing a nearly athermal behaviour are expected for light polarizations E || X and E || Z. In particular, these polarizations are of interest in the case of Yb doping of oxoborates as they provide access to higher absorption and stimulated emission cross-sections. Despite the fact that dn/dT coefficients are negative, a positive thermal lens is expected for X-cut and Z-cut YCOB and GdCOB crystals doped with Yb^{3+}, Er^{3+} or Nd^{3+} ions. This is crucial in particular for the potential application in microchip lasers.

Acknowledgments

This work was partially supported by The National Natural Science Foundation of China (Fund No. 51402268).

Репозиторий БНТУ

#233231 - $15.00 USD Received 27 Jan 2015; revised 31 Mar 2015; accepted 3 Apr 2015; published 15 Apr 2015